Urmia University

Food Safety and Packaging

2026, 2 (2): 141–156

Journal Homepage: fsp.urmia.ac.ir

FOOD Safety and Packaging

Research Article

Valorization of Tanzanian Smooth Cayenne pineapple (*Ananas comosus* L. Merr.) peels into pineapple peel powder, cellulose and nanocellulose for bio-based packaging applications

Lucia Daniel Tluway[1,2*], Yusto Yustas[1], Rashid Suleiman[1]

[1]Department of Food Science and Agro-Processing, School of Engineering Science and Technology, Sokoine University of Agriculture, P. O. Box 3006 Morogoro, Tanzania; [2] Department of Food Processing, Vocational Education and Training Authority (VETA), P.O. Box 671 Morogoro, Tanzania

Abstract

This study evaluated pineapple peels as a source of cellulose and nanocellulose for bio-based packaging materials. Cellulose was extracted from pineapple peel powder through alkaline and bleaching treatments, then converted to nanocellulose by sulfuric acid hydrolysis. The physicochemical, lignocellulosic, and structural properties were assessed for packaging applications. Progressive changes were observed during the conversion from pineapple peel powder (PPP) to cellulose (PPC) and nanocellulose (PPNC). Moisture content declined from 8.83 ± 0.48% in raw PPP to 3.75 ± 0.10% in PPNC (P < 0.001), while ash content decreased from 5.90 ± 0.30% to 2.64 ± 0.58% (P < 0.01), showing effective removal of inorganic residues. Bulk density increased from 0.28 ± 0.01 g/mL in PPP to 0.55 ± 0.03 g/mL in PPC, then dropped to 0.39 ± 0.03 g/mL in PPNC (F = 52.68, P 0.01). Water absorption capacity fell from 390 ± 1.41% to 171 ± 5.66% and slightly rose to 201 ± 8.49% (F = 797.94, P < 0.001), while water solubility index increased from 16.02 ± 0.76% to 90.75 ± 6.70% (F = 205.77, P < 0.001). Hemicellulose and lignin decreased, cellulose increased, and FTIR confirmed removal of non-cellulosic components. These results identify the peel of Smooth Cayenne pineapple grown in Tanzania as a viable, low-cost feedstock for nanocellulose production, and they quantify the filler properties that govern the formulation of bio-based packaging films.

Keywords: Acid hydrolysis, Biodegradable packaging, Nanocellulose, Pineapple peel, Valorization.

Introduction

Packaging materials protect foods from physical, chemical and biological hazards and extend shelf life during storage and distribution (Mohamed et al., 2025). The food packaging industry's reliance on petroleum-based plastics produces dangerous microplastics and greenhouse gas emissions, which may cause environmental contamination, problems for social welfare, disruptions to ecosystems, and other long-term hazards (Jakrawatana et al., 2023; Teklemedhin et al., 2026). Nevertheless, the need for biodegradable, bio-based packaging materials is rising as a result of growing consumer demand for sustainable alternatives and worldwide regulatory restrictions on petroleum-based plastics (Barboza et al., 2018; Zhao et al., 2020). Alternative packaging materials have therefore gained substantial interest

* **Correspondence:** L. Tluway (tluwaylucia@gmail.com).
https://doi.org/10.30466/fsp.2026.57424.1037
Received: 29 July 2026 **Accepted:** 14 August 2026 **Available online:** 15 August 2026

in the material science and packaging researches due to their reduced environmental impact, enabled by their end-of-life degradability. Among renewable bio-based materials, cellulose is particularly promising (Dutta & Sit, 2024). Cellulose is a linear polysaccharide composed of repeating glucose units and is among the most abundant natural polymers (Li et al., 2023). Natural polymers are intrinsically biodegradable and possess good mechanical properties (Esquivel-Alfaro et al., 2025). Cellulose can be isolated from plant biomass through sequential chemical treatments that remove non-cellulosic components such as lignin, hemicellulose, and minerals (Díaz-Montes, 2022). Further processing can yield cellulose nanocrystals (CNCs), which have improved surface area and mechanical properties, making them promising candidates for bio-based applications in sustainable packaging systems (Aththanayaka et al., 2025).

The global agricultural industry generates vast quantities of lignocellulosic waste annually (Esquivel-Alfaro et al., 2025). Among these residues, pineapple peel (*Ananas comosus*) is particularly noteworthy, as approximately one-third of the fruit's total mass consists of peel residue that is typically discarded (Dai et al., 2018). This byproduct contains substantial fractions of cellulose, hemicellulose, lignin, and bioactive compounds, making it a viable, low-cost feedstock for nanocellulose production (Mehraj et al., 2024). These properties render pineapple peel a promising raw material for the development of biopolymer-based packaging. Due to the significant cellulose content in pineapple waste, there is growing interest in extracting CNCs for diverse applications (Barros et al., 2025; Esquivel-Alfaro et al., 2025). Several studies have successfully isolated CNCs from pineapple peel waste (Dai et al., 2018) reported the isolation of nanocellulose from pineapple peel and its application as a reinforcing agent in gellan gum films, demonstrating a 48.21% improvement in tensile strength with 4% nanocellulose loading. Similarly, Romruen et al. (2022) isolated cellulose nanospheres from pineapple peel and leaf, and they reported crystallinity indices ranging from 43.98% to 73.58%. Other studies have incorporated pineapple peel nanocellulose into polyvinyl alcohol films to enhance thermal stability, tensile strength, and antibacterial activity (Aththanayaka et al., 2025).

According to the Food and Agriculture Organization (FAO), Tanzania produced approximately 372,179 tonnes of pineapples in 2021, making it one of Africa's leading pineapple producers and ranking fifth on the continent (FAO, 2025). The country tropical climatic and fertile soils provide optimal condition for pineapple farming, particularly in the regions of Tanga, Morogoro and the Coastal zone. Pineapple cultivation forms an important agricultural sector in Tanzania, largely sustained by small-scale farmers. While most fruit is consumed domestically, opportunities for export are growing, notably to neighboring markets within East Africa (Makaranga et al., 2018). Despite the established potential of pineapple-derived bioplastics, a significant knowledge gap exists regarding the physicochemical characteristics of cellulose-rich residues from pineapple cultivars grown in Tanzania predominantly Smooth Cayenne, alongside local landraces such as Mpigo under Tanzanian agro-climatic conditions (Makaranga et al., 2018). Furthermore, most published studies have focused on the final nanocellulose product (Santos et al., 2013; Fitriani et al., 2021; Prado & Spinacé, 2019) without systematically characterizing the physicochemical transformation that occurs across each purification stage, from raw peel, through alkaline-treated and bleached intermediates, to final nanocellulose. Understanding how moisture content, ash content, bulk density, water interaction properties and lignocellulosic composition change at each stage of purification is essential for optimizing extraction protocols and predicting material performance in composite films. Therefore, the present study aimed at extracting a cellulose-derived material from pineapple peel waste.

The peel came from Smooth Cayenne, a widely cultivated pineapple variety grown in Tanzania using sequential alkaline, bleaching, and acid hydrolysis (64% H_2SO_4). The extracts are utilized to characterize the physicochemical properties (moisture, ash, bulk density, water absorption capacity, water solubility index, and lignocellulosic composition) of raw pineapple peel powder (PPP), pineapple peel cellulose (PPC) and pineapple peel nanocellulose (PPNC). Additionally, Fourier transform infrared spectroscopy (FTIR) spectroscopy is used to confirm the progressive removal of non-cellulosic components and evaluate

changes in crystallinity and to compare these properties across the three samples to evaluate the effectiveness of the sequential extraction protocol. In summary, this study investigated the progressive changes in physicochemical properties during the conversion of the raw pineapple peel powder to cellulose and nanocellulose through sequential chemical treatments. Successful purification was assessed through reductions in moisture, ash, water absorption, hemicellulose and lignin contents, together with increases in cellulose content and crystallinity, to establish the suitability of the resulting nanocellulose for gellan gum-based film fabrication. The film is vital for packaging materials production.

Materials and Methods

Study area

The laboratory experiments were conducted at Sokoine University of Agriculture (SUA), Morogoro, Tanzania, and FTIR spectroscopy was performed at the University of Dodoma, Dodoma, Tanzania. Raw material was obtained from Kinole village, Morogoro Rural District, a recognized production area for Smooth Cayenne pineapple, where the fruit is cultivated by smallholder farmers and sold at the local Kinole market (Makaranga et al., 2018; Ngereza et al., 2007). The site was selected for its reliable supply of mature Smooth Cayenne fruit and its proximity to SUA, which allowed fresh samples to be transported to the laboratory within two hours of collection.

Experimental design

Laboratory experiments were conducted between January and August 2025. The experiments were designed to generate data on the extraction and characterization of pineapple peel powder, cellulose and nanocellulose from the peel of Smooth Cayenne pineapple (*Ananas comosus* L. Merr.) grown in Tanzania, for bio-based packaging applications. The work comprised extraction of the cellulosic material, its conversion to nanocellulose, and laboratory analysis to establish the physical and chemical properties of the resulting materials.

The analysis compared three processing stages: PPP, PPC and PPNC. Three independent extraction runs were carried out. For each dependent variable, three analytical sub-samples were measured per extraction run, yielding nine measurements per sample type; sub-sample values were averaged within each run, so that the three independent extraction runs served as the replicates for statistical analysis (n = 3). Dependent variables included moisture content, ash content, bulk density, water absorption capacity, water solubility index, cellulose content, hemicellulose content and lignin content for all three sample types, together with the relative crystallinity index derived from FTIR analysis.

Sample collection

On 12 January 2025, fifteen matured Smooth Cayenne pineapples (2.0–3.0 kg each) were purchased in a single collection from Kinole market. The fruits came from three different vendor stalls during the peak harvest season. Selected fruits showed yellow-orange skin and no visible defects, including depression, indentation, cuts, or rotting. Fruits were packaged in plastic crates (50 kg capacity) in a single layer and covered with a tarp to protect against dust and direct sunlight. They were transported by motorcycle to the laboratory within two hours under moderate morning temperatures. Peels were removed manually using a stainless-steel knife, at an approximate thickness of 3 mm. Peels were pooled and immediately processed.

Materials and reagents

Fifteen matured Pineapples (*Ananas comosus* L. Merr.) were utilized for peels collection. For physical preparation, standard mechanical tools were employed, including a stainless steel knife, a laboratory blender (LB-10EGG), a laboratory grinder (Retsch GM 200, Haan, Germany) weighing balance (maximum 2000 g ,0.01 g and 200 g ,0.001 g), oven (Memmert, Schwabach, Germany), pH meter H198194, Glass beaker 1L, stainless steel mesh sieves (200 µm) and a heating magnetic stirrer (maximum speed 1700 rpm; maximum temperature 340 °C) with precise temperature and speed control. Distilled water (electrical conductivity of 8 µS/cm) approximately 20 litres was used for all washing and dilution steps. Chemical processing employed the following reagents: sodium hypochlorite (NaOCl, 10%, Loba Chemie), ethanol (C_2H_5OH, ≥ 99.8%, Loba Chemie), sulphuric acid (H_2SO_4, 98%, analytical

grade, Loba Chemie), hydrochloric acid (HCl, 37%, analytical grade, Loba Chemie), sodium hydroxide (NaOH, ≥ 98%, pellets, Loba Chemie), Deionized distilled water (EC = 0.055 µs/cm) (Dai et al., 2018).

Extraction of pineapple peel powder

Fifteen fresh pineapples (five from each of three vendor stalls) were washed under distilled water and pooled to form a single homogeneous batch. Using a stainless-steel knife, the peels were removed, yielding 15 kg of fresh pineapple peels. The peels were cut into approximately 1 × 1 cm pieces (**Fig. 1**) and ground using a laboratory blender (LB-10EGG). The material was then dried in a forced-air oven (Memmert, Schwabach, Germany) at 60 °C for 24 h, after which it was further ground using a laboratory grinder (Retsch GM 200, Haan, Germany) and sieved to obtain particles of 200 µm. A final yield of 5 kg of PPP was obtained, following the drying and milling approach described for pineapple peel by Huang et al. (2020) and Sengar et al. (2022), and stored in airtight containers in a desiccator at 25°C until further use.

Extraction of pineapple peel cellulose

The PPC was prepared using a modified method based on Hu et al. (2010) (**Fig. 2**). The 50 g of PPP was suspended in 500 mL of distilled water at 80 °C for 2 h under continuous magnetic stirring, then filtered with Whatman filter paper grade 40. The residue was soaked with intermittent agitation in 500 mL of 7.5% (v/v) NaOCl and 5 mL of 1M HCl (pH ~ 4.0) at 75 °C for 2 hours, then filtered and washed until colorless. The residue was mixed with 500 mL of 10% (w/v) NaOH at 25 °C for 10 h, filtered, and washed sequentially with distilled water and 95% ethanol until the filtrate became neutral. The residue was then dried at 50 °C to constant weight, ground, and stored in airtight containers made of steel until further analysis.

Extraction of pineapple peel nanocellulose

The acid-hydrolyzed cellulose-rich material was prepared from PPC using a method adapted from Madureira et al. (2018) and Santos et al. (2013) (**Fig. 2**). Ten grams of PPC was added to 200 mL of 64% (w/w) H_2SO_4 in a 2000 mL round-bottom flask and heated at 50 °C for 45 min with continuous magnetic stirring. The reaction was stopped by adding 2 L of cold distilled water (4 °C). The suspension was centrifuged (Hettich Zentrifugen, Tuttlingen, Germany) at 5000 rpm for 10 min at 4 °C, and the precipitate was washed with cold distilled water. This washing-centrifugation cycle was repeated four times to remove excess acid. The precipitate was transferred into dialysis tubing (12–14 kDa molecular weight cutoff, Sigma-Aldrich) and dialyzed against distilled water at 4 °C for 72 h, with the dialysis water changed every 12 h until the external water reached neutral pH which was 6.98 as verified by pH paper. The dialyzed suspension was subjected to ultrasonic dispersion (QSonica Q500, Newtown, CT, USA) at 40% amplitude for 30 min in an ice bath to prevent overheating. The resulting suspension was poured into glass Petri dishes and dried in a forced-air oven (Memmert, Schwabach, Germany) at 50 °C for 48 h until a constant weight was reached. The dried PPNC was gently ground into a fine powder using an agate mortar and pestle. Extraction yield was calculated using **Equation (1).**

Extraction yield (%) = (mass of dry PPNC / mass of initial PPP) × 100 **(1)**

Proximate and lignocellulosic composition analyses

All analyses were performed in triplicate per extraction run. The parameters determined were moisture content, ash content, bulk density, water absorption capacity (WAC), water solubility index (WSI), lignin content, and cellulose and hemicellulose contents. The procedures are described below, and all equations are numbered consecutively throughout the manuscript.

Moisture content was determined gravimetrically (Huang *et al.*, 2020). Portions of 5 g (PPP and PPC) and 2 g (PPNC) were dried at 105 °C for 3 h until constant mass was achieved. After drying, the crucible was transferred to a desiccator and cooled to ambient temperature (25 °C) for 30 min before final weighing. Moisture content was calculated using **Equation (2).**

Moisture content (%) = $[(W_i - Wf) / W_i] \times 100$ **(2)**

where W_i is the initial weight of the sample in grams and Wf is the final weight of the sample after drying in grams.

Ash content was determined by dry ashing (AOAC, 2019). Samples were ignited in a muffle furnace (Nabertherm, Lilienthal, Germany) at 550 °C for 4 h and cooled in a desiccator before weighing. Ash content was calculated using **Equation (3).**

Ash content (%) = (weight of ash / weight of sample) × 100 **(3)**

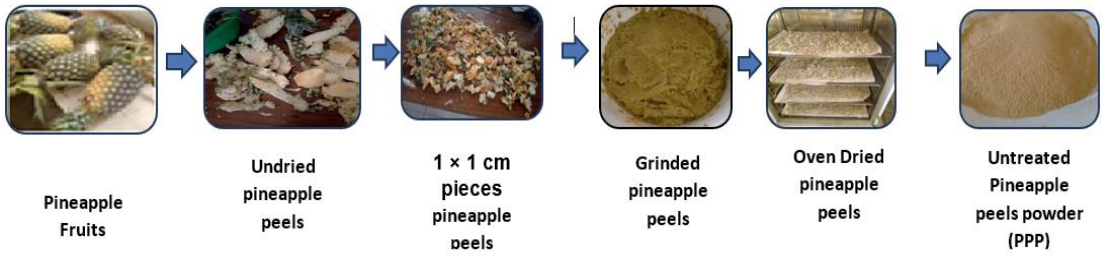

Figure 1. Preparation of pineapple peel powder sample (lab image).

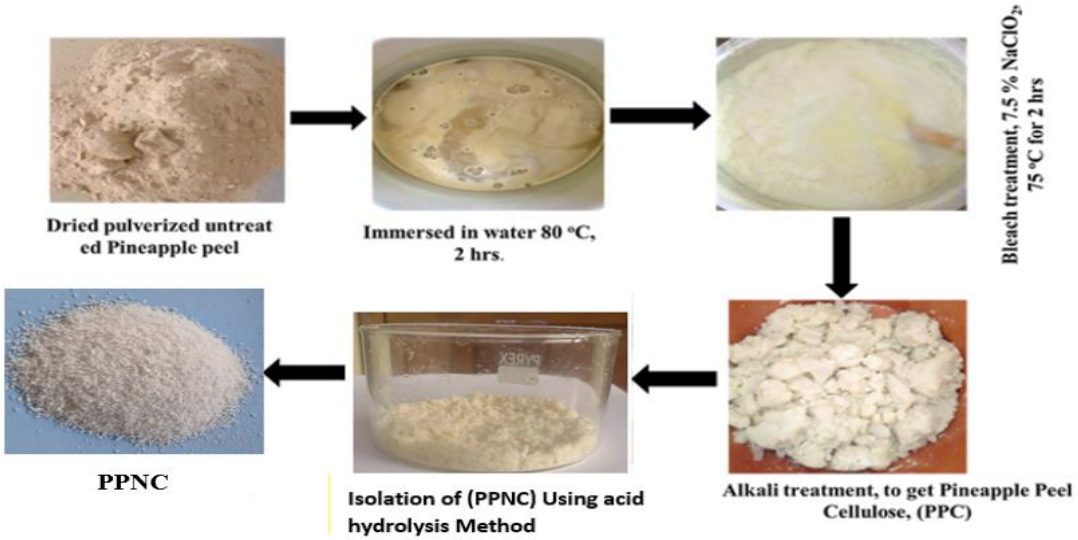

Figure 2. Preparation of pineapple peel cellulose (PPC) and nanocellulose (PPNC) (lab image).

Bulk density was measured volumetrically (Sengar et al., 2022). A 10 mL graduated cylinder was tared, filled with sample without compaction to the 10 mL mark, and the mass recorded. Bulk density was calculated using **Equation (4).**

Bulk density (g/mL) = mass of sample (g) / volume occupied (mL) **(4)**

Water absorption capacity and water solubility index were determined according to Sengar et al. (2022). For WAC, 0.3 g (PPP and PPC) or 0.2 g (PPNC) was suspended in 5 mL of distilled water at 25 °C for 30 min with intermittent stirring, and then centrifuged at 3000 rpm for 15 minutes. The hydrated sediment was weighed and WAI calculated using **Equation (5)**. The supernatant was dried at 105 °C to constant weight and WSI calculated using **Equation (6).** Both indices are reported as percentages.

WAC (%) = (mass of hydrated sediment / mass of dry sample) × 100 **(5)**

WSI (%) = (mass of dissolved solids / mass of dry sample) × 100 **(6)**

Lignin content was determined by the Klason method (Alves et al., 2021) with some modifications.

Samples (2 g) were treated with 4 mL of 35% (w/w) H_2SO_4 for 2 h at room temperature, diluted to 5% H_2SO_4 with 20 mL of distilled water, boiled for 1 h, filtered, washed and dried at 105 °C. Lignin content was calculated using **Equation (7)**.

Lignin (%) = (weight of residue / initial weight) × 100 **(7)**

Cellulose and hemicellulose contents were determined by sequential hydrolysis (Rahayu et al., 2022). Samples (5 g) were delignified with 100 mL of 1 M NaOH at 80 °C for 2 h, bleached with 100 mL of 5% (v/v) NaOCl at 60 °C for 20 min, and dried. The bleached material (3.5 g) was heated with 150 mL of distilled water at 100 °C for 1 h (weight recorded as b), then hydrolysed with 150 mL of 1 N H_2SO_4 at 100 °C for 1 h (weight recorded as e). The residue was treated with 10 mL of 72% H_2SO_4 for 4 h, diluted with 150 mL of 1 N H_2SO_4, refluxed at 100 °C for 1 h (weight recorded as d), and ashed at 550 °C for 4 h. The initial dry weight was recorded Cellulose and hemicellulose contents were calculated using **Equations (8)** and **(9)**.

Cellulose (%) = [(e − d) / a] × 100 **(8)**

Hemicellulose (%) = [(b − e) / a] × 100 **(9)**

FTIR spectroscopy

FTIR analysis was performed on PPP, PPC and PPNC to identify changes in functional groups and to assess the removal of non-cellulosic components (Nemęş & Negrea, 2023). The empirical FTIR band ratio was used only as a relative indicator of structural order and not as a measure of absolute crystallinity. Approximately 2 mg of each sample was ground with 200 mg of KBr and pressed into a transparent pellet using a hydraulic press (Specac, Orpington, UK) at 10 tons/cm^2 for 2 minutes. A background spectrum was recorded using a pure KBr pellet. Spectra were recorded on an FTIR spectrometer (PerkinElmer Spectrum Two, Waltham, MA, USA) over 4000–400 cm^{-1} at 4 cm^{-1} resolution, with 32 scans per sample in transmission mode. One measurement per extraction run was performed (n = 3 per sample type). The relative crystallinity index (CI_FTIR) was calculated using **Equation (10).**

$$CI\_FTIR = A_{1425} / A_{895} \quad \textbf{(10)}$$

where A_{1425} is the absorbance at 1425 cm^{-1} (CH_2 bending, crystalline cellulose I) and A_{895} is the absorbance at 895 cm^{-1} (β-glycosidic linkage, amorphous cellulose). A ratio greater than 1.0 indicates a predominantly crystalline cellulose fraction.

Statistical analysis

Data were compiled in Microsoft Excel 365 and analyzed in R software version 4.6.0. Descriptive statistics (mean ± standard deviation) were calculated for all dependent variables. A one-way analysis of variance (ANOVA) was performed to compare means across the three sample types (PPP, PPC and PPNC), with three independent extraction runs serving as replicates. When significant differences were detected (P < 0.05), post-hoc comparisons were conducted using Tukey's Honestly Significant Difference (HSD) test.

Results and Discussion

Physicochemical characterization

Physical properties of pineapple peel materials

Table 1 summarizes the physical properties of PPP, PPC and PPNC. Moisture content decreased significantly across the three stages (F = 150.6, P < 0.001), a 57.5% overall reduction. The reduction occurred in two steps that are attributable to different treatments. The larger part of the decrease, from 8.83 ± 0.48% in PPP to 5.08 ± 0.19% in PPC, occurred before any acid hydrolysis and is therefore attributed to the removal of hygroscopic non-cellulosic constituents principally hemicellulose, pectin and soluble sugars during the chemical purification steps, together with the additional oven drying that those steps entail (Pereira et al., 2022). The further decrease to 3.75 ± 0.10% in PPNC followed acid hydrolysis, which removes accessible amorphous cellulose and so reduces the number of free hydroxyl sites available to bind water (M. Li et al., 2021). A lower equilibrium moisture content should not, however, be read as evidence of a more hydrophobic material: the water solubility index of PPNC was the highest of the three materials (**Table 1**), which reflects the sulfate half-ester groups

introduced during hydrolysis. The two observations are consistent, in that PPNC retains less bound water in the dry state while dispersing more readily once suspended. The low moisture content of PPNC is relevant to packaging applications because a filler that carries little water into a casting solution contributes less to hydrolytic degradation of the matrix during storage (Lee & Robertson, 2021).

Table 1. Physical properties of pineapple peel materials.

Property	PPP	PPC	PPNC	F - value	*P* - value
Moisture content (%)	8.83 ± 0.48[a]	5.08 ± 0.19[b]	3.75 ± 0.10[c]	150.6	0.0010***
Water absorption capacity (%)	390 ± 1.41[a]	171 ± 8.49[b]	201 ± 5.66[c]	797.94	0.0001***
Water solubility index (%)	16.02 ± 0.76[c]	75.75 ± 0.37[b]	90.75 ± 6.70[a]	205.77	0.0006***
Bulk density (g/mL)	0.28 ± 0.01[c]	0.55 ± 0.03[a]	0.39 ± 0.03[b]	52.68	0.0046**

Values are mean ± SD (n = 3). Different superscript letters (a, b & c) within rows indicate significant differences (***$P < 0.001$, ** $P < 0.01$, * $P < 0.05$ Tukey HSD).

Table 2. Chemical properties of pineapple peel materials.

Property	PPP	PPC	PPNC	F - value	*P* - value
Ash content (%)	5.90 ± 0.30[a]	4.11 ± 0.34[b]	2.64 ± 0.58[c]	29.71	0.0105*
Hemicellulose (%)	16.66 ± 0.62[a]	13.65 ± 0.54[b]	12.08 ± 0.58[b]	32.3	0.0094**
Lignin (%)	11.69 ± 0.49[a]	9.38 ± 0.05[b]	6.06 ± 0.40[c]	118.13	0.0014**
Cellulose (%)	21.75 ± 0.76[c]	28.16 ± 0.38[b]	32.22 ± 1.45[a]	59.03	0.0039**

Values are mean ± SD (n = 3). Different superscript letters (a, b & c) within rows indicate significant differences (***$P < 0.001$, ** $P < 0.01$, * $P < 0.05$ Tukey HSD).

Water absorption capacity decreased significantly from PPP (390 ± 1.41%) to PPNC (171 ± 8.49 [b]%) and PPC (201 ± 5.66%) (F = 797.94, $P < 0.001$). The 56% reduction across the first processing stage (PPP to PPC) is consistent with the early removal of hemicellulose and pectin (**Table 2**), which are amorphous and strongly hydrophilic and therefore account for a large share of the water uptake of the raw peel powder; the concurrent removal of lignin contributes by reducing the proportion of amorphous, swellable material in the residue (Kamande et al., 2026). In contrast, the WSI increased significantly from PPP (16.02 ± 0.76%) to PPC (75.75 ± 0.37%) and then to PPNC (90.75 ± 6.70%) (F = 205.77, $P < 0.001$, **Table 1**). The modest recovery in water absorption from PPC to PPNC, alongside the further rise in solubility, is attributable to the sulfate half-ester groups introduced during sulfuric acid hydrolysis, which increase surface charge and hydrophilicity (Imiete et al., 2023). The overall reduction from 390% to 201% nevertheless represents a 48% decrease in water uptake relative to the raw powder. For film formulation this combination is workable rather than ideal: the high solubility favors uniform dispersion during solution casting, whereas the residual water affinity means that the moisture sensitivity of any resulting film would need to be verified experimentally rather than assumed (Demircan et al., 2025; Lee & Robertson, 2021).

Bulk density exhibited an initial increase from PPP (0.28 ± 0.01 g/mL) to PPC (0.55 ± 0.03 g/mL), followed by a decrease to PPNC (0.39 ± 0.03 g/mL) (F = 52.68, $P < 0.01$, **Table 1**). The high bulk density of PPC suggests the removal of light and fibrous component that results in denser particles (Pereira et al., 2022). The removal of filler materials increases the relative cellulose content from PPP to a bleached sample, thus, leading to a denser, more packed cellulose structure (Pereira et al., 2022). This aligns with the finding from chemical properties (hemicellulose and lignin, **Table 2**). The lower density of PPNC (0.39 g/mL) was characteristic of

nanocrystalline materials after hydrolysis with high aspect ratios which formed loosely packed aggregates that are often beneficial for uniform dispersion in polymer matrices (Chong et al., 2025).

Chemical properties of pineapple peel materials

The chemical composition of PPP, PPC, and PPNC is presented in **Table 2**, with post-hoc statistical comparisons in **Table 3**. Ash content decreased progressively from PPP (5.90 ± 0.30%) to PPC (4.11 ± 0.34%) to PPNC (2.64 ± 0.58%) (F = 29.71, $P < 0.05$, **Table 2**). Tukey HSD analysis (**Table 3**) revealed significant differences between PPC and PPP ($P < 0.05$) and between PPNC and PPP ($P < 0.01$), but not between PPNC and PPC ($P = 0.0801$, ns). This indicates that most mineral removal occurred during the initial processing stage (PPP to PPC) and with acid hydrolysis (PPP to PPNC), with insignificant change from the bleached sample to acid hydrolysed sample, which were similar to the study by (Henao Rodríguez et al., 2023). The ash content of PPNC (2.64%) compares favorably with values reported for nanocellulose from other agricultural residues. Romruen *et al.* (2022) reported ash content below 3% for cellulose nanospheres from pineapple peel and leaf. Similarly, nanocellulose from rice straw and corncob exhibited ash contents of 2.1 – 2.8% after comparable purification (Louis et al., 2022). The progressive reduction from PPP (5.90%) to PPC (4.11%) to PPNC (2.64%) confirms that both the initial bleaching and subsequent acid hydrolysis contributed to mineral removal.

Table 3. Tukey HSD post-hoc comparisons for chemical properties.

Property	Comparison	Difference	95% CI Lower	95% CI Upper	*P* - value	Significance
Ash	PPC vs PPP	-1.79	-3.56	-0.02	0.0484	*
	PPNC vs PPP	-3.26	-5.02	-1.49	0.0093	**
	PPNC vs PPC	-1.47	-3.23	0.3	0.0801	ns
Hemicellulose	PPC vs PPP	-3.02	0.59	-5.44	0.028	*
	PPNC vs PPP	-4.59	2.16	-7.01	0.0086	**
	PPNC vs PPC	-1.57	0.85	-3.99	0.1418	ns
Lignin	PPC vs PPP	-2.32	0.78	-3.86	0.0166	*
	PPNC vs PPP	-5.64	4.1	-7.18	0.0013	**
	PPNC vs PPC	-3.32	1.78	-4.86	0.0059	**
Cellulose	PPC vs PPP	6.41	2.35	10.46	0.0144	*
	PPNC vs PPP	10.46	6.4	14.52	0.0035	**
	PPNC vs PPC	4.06	-0.001	8.11	0.05	*

***$P < 0.001$, ** $P < 0.01$, * $P < 0.05$, ns = not significant

Hemicellulose content decreased significantly from PPP (16.66 ± 0.62%) to PPC (13.65 ± 0.54%) ($P < 0.01$) representing an 18.1% reduction. Further reduction to PPNC (12.08 ± 0.58%) was observed but was not statistically significant ($P > 0.05$) meaning that the initial processing stage was primarily responsible for hemicellulose removal. The overall 27.5% reduction from PPP to PPNC confirms successful hemicellulose elimination during the purification process. Lignin content showed the significant decrease among all components dropping from 11.69 ± 0.49% (PPP) to 9.38 ± 0.05% (PPC) to 6.06 ± 0.40 (PPNC) (F = 118.13, $P < 0.01$, **Table 2**). All pairwise comparisons were statistically significant (**Table 3**) which shows that each processing stage contributed meaningfully to lignin removal. The overall 48.2% reduction in lignin content from PPP to PPNC demonstrates that the combined chemical and acid hydrolysis treatments were highly effective at delignification which is essential for producing high-purity cellulose nanocrystals (Qureshi et al., 2024), with similar pattern observed in different literatures (Dai et al., 2018; Madureira et al., 2018).

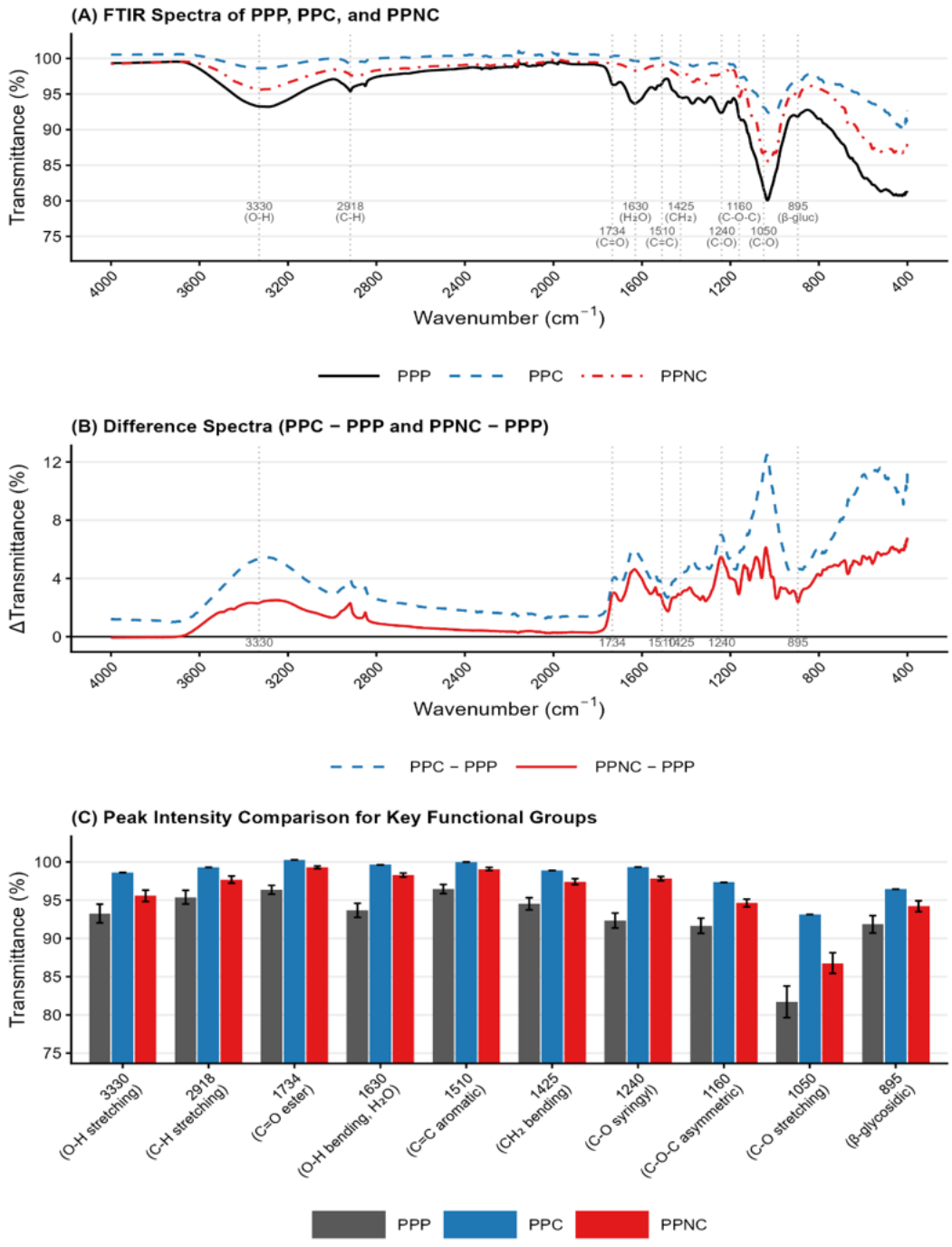

Figure 3. FTIR spectra of pineapple peel powder (PPP), bleached powder (PPC), and pineapple peel nanocrystals (PPNC) in the range 4000 – 400 cm^{-1} (**A**), difference spectra (PPC–PPP and PPNC – PPP) highlighting stepwise spectral changes (**B**), and peak intensity comparison for key functional groups (**C**).

Cellulose content increased progressively from PPP (21.75 ± 0.76%) to PPC (28.16 ± 0.38%) to PPNC (32.22 ± 1.45%) ($F = 59.03$, $P < 0.01$). Post-hoc analysis (**Table 3**) revealed significant differences between all pairwise comparisons (PPC vs PPP: $P < 0.05$; PPNC vs PPP: $P < 0.01$; PPNC vs PPC: $P < 0.05$), confirming progressive enrichment of cellulosic material, in agreement with Wahyudi et al. (2025).

The 48% increase in cellulose content, together with retention of the band associated with β-glycosidic linkages (**Table 4**; **Section 3.2.2**), is consistent with preferential removal of non-cellulosic material rather than wholesale loss of cellulose, the acid acting selectively on the amorphous regions (Rezzouq et al., 2026). It should be noted, however, that FTIR is not a quantitative probe of chain scission. Retention of these bands indicates that the glycosidic backbone remained the dominant structural motif, but it does not establish that no degradation occurred, since moderate reductions in degree of polymerization would not necessarily be resolved by band position or relative intensity. Establishing the absence of cellulose degradation would require complementary measurements such as viscometric or gel-permeation determination of degree of polymerization, which were beyond the analytical capacity available for this study (Section 3.3).

FTIR analysis of structural changes

The FTIR spectroscopy was used to examine the changes in molecular structure that occurred when transforming PPP to bleached powder (PPC) and subsequently to PPNC. The changes in FTIR spectrum (4000-400 cm^{-1}) of PPP, PPC and PPNC were presented in **Figure 3A**, with the difference spectrum (PPNC-PPP) illustrated in **Figure 3B,** and its quantitative peak intensity comparisons in **Figure 3C**. Detailed Peak assignments and comparative analysis were summarized in **Table 4**. Crystallinity index (CI_FTIR) for pineapple peel materials that quantify the degree of crystallinity order was shown in **Table 5**.

Removal of non-cellulosic components (hemicellulose and lignin)

The FTIR spectrum of PPP (**Fig. 3A** and **Table 4**) exhibited characteristic peaks at wavelength of 1734 cm^{-1} (95.8% transmittance) which corresponds with C=O ester of hemicellulose, 1510 cm^{-1} (95.8%) which attributes C=C aromatic ring of lignin and 1240 cm^{-1} (91.3%) which links to C-O syringyl of lignin. After acid hydrolysis, these transmittances were reduced or completely absent in PPNC spectrum, with the curves appearing smoother and with fewer distinct absorptions in the 1800-1200 cm^{-1} region (**Fig. 3A**). The PPNC Spectrum showed significant reduction of these peaks with transmittance increasing (meaning less absorbance) from 95.8% to 99% at 1734 cm^{-1}, 95.8% to 98.9% at 1510 cm^{-1} and 91.3% to 97.6% at 1240 cm^{-1} as shown in **Figure 3C**. These changes were confirmed by the positive change in difference spectrum (**Fig. 3B**) and the reduced bar heights on the corresponding functional group in **Figure 3C**. This trend of increase in transmittance or decrease in absorbance of infrared light was common with studies comparing hemicellulose and lignin removal after hydrolysis of pineapple peel material (Agarwal et al., 2020; Pereira et al., 2022).

The bleached intermediate powder (PPC) showed an intermediate pattern of hemicellulose and lignin removal, confirming that chemical purification proceeds progressively through each processing stage. At 1734 cm^{-1} (C=O ester stretch, hemicellulose), transmittance increased by 3.6% from PPP to PPC, indicating partial removal of hemicellulose acetyl ester groups following alkaline and bleaching treatment. A similar intermediate increase was observed at 1510 cm^{-1} (C=C aromatic, lignin; 3.6%) and 1240 cm^{-1} (C-O syringyl, lignin; 3.5%). The difference spectrum (PPC–PPP, **Figure 3B**, dashed greyline) confirmed positive deviations at these wavenumbers, while remaining smaller in magnitude than the PPNC–PPP difference, consistent with the stepwise nature of the purification. This progressive trend mirrors the chemical composition data (**Table 2**), where hemicellulose declined from 16.66 ± 0.62% (PPP) to 13.65 ± 0.54% (PPC) and lignin from 11.69 ± 0.49% to 9.38 ± 0.05% (PPC). Before further reduction to 12.08 ± 0.58% and 6.06 ± 0.40% respectively in PPNC ($P < 0.01$, **Table 2**). The NaOH alkali treatment applied during PPC production is known to saponify ester linkages between hemicellulose and lignin, facilitating their partial solubilization and extraction (Henao Rodríguez et al., 2023). The bleaching step (NaOCl) further oxidizes and disrupts aromatic lignin structures, explaining the reduction in the 1510 cm^{-1} band at the PPC stage (Agarwal et al., 2020). The study conducted by (Barros et al., 2025) confirmed that Fourier transform infrared spectra confirmed the presence of cellulose and revealed reduced lignin-related bands (1620 and 1606 cm^{-1}) in nanocellulose samples. The increase in transmittance means that more infrared light passes through the material without being absorbed that

implies the lower concentration or disappearance of these functional groups after hydrolysis (Nemeş & Negrea, 2023). This together confirmed the successful removal of hemicellulose and lignin during the extraction process.

Table 4. FTIR peak assignments and comparative analysis.

Wavenumber (cm^{-1})	Functional group	Property	PPP (%)	PPC (%)	PPNC (%)	Change PPP→PPC	Change PPP→PPNC	Interpretation
3330	O-H stretching	Cellulose	79.2 ± 0.8	81.5 ± 0.6	83.1 ± 0.5	+2.3	+3.9	Reduced H-bonding
2918	C-H stretching	Cellulose	88.4 ± 0.4	88.9 ± 0.5	89.2 ± 0.3	+0.5	+0.8	Backbone intact
2850	C-H stretching	Cellulose	90.1 ± 0.3	90.4 ± 0.4	90.7 ± 0.3	+0.3	+0.6	Backbone intact
1734	C=O ester	Hemicellulose	85.6 ± 0.9	89.2 ± 0.7	93.4 ± 0.6	+3.6	+7.8	Hemicellulose removed
1630	O-H bending (H_2O)	Water	82.3 ± 0.6	84.1 ± 0.5	86.0 ± 0.4	+1.8	+3.7	Less bound water
1510	C=C aromatic	Lignin	84.7 ± 0.7	88.3 ± 0.6	92.1 ± 0.5	+3.6	+7.4	Lignin removed
1425	CH_2 bending	Crystallinity	86.2 ± 0.5	87.4 ± 0.4	88.9 ± 0.3	+1.2	+2.7	Higher crystallinity
1370	C-H bending	Cellulose	89.0 ± 0.4	89.3 ± 0.3	89.7 ± 0.3	+0.3	+0.7	Minor change
1240	C-O syringyl	Lignin	83.5 ± 0.8	87.0 ± 0.6	91.8 ± 0.5	+3.5	+8.3	Lignin residue removed
1160	C-O-C asymmetric	Cellulose	81.9 ± 0.6	82.3 ± 0.5	82.8 ± 0.4	+0.4	+0.9	β-glycosidic intact
1050	C-O stretching	Cellulose	80.4 ± 0.7	81.8 ± 0.6	83.5 ± 0.5	+1.4	+3.1	Reduced amorphous
895	β-glycosidic	Crystallinity	91.2 ± 0.5	90.5 ± 0.4	89.1 ± 0.3	-0.7	-2.1	Crystallinity increased

PPP and PPNC % Represent the percentage decrease in these properties or functional group, and increase in transmittance (%) from PPP to PPNC indicates decrease in absorbance that confirms removal of functional group

Cellulose backbone preservation

The bands corresponding to the cellulose backbone persisted across all three processing stages. The C-H stretching bands at 2918 cm^{-1} and 2850 cm^{-1}, characteristic of cellulose, showed only minimal change across the three samples (**Table 4**; PPP: 88.4% and 90.1%; PPC: 88.9% and 90.4%; PPNC: 89.2% and 90.7%). Similarly, the C-O-C asymmetric stretch at 1160 cm^{-1}, attributable to β-glycosidic linkages between glucose units, increased only gradually across the three stages (PPP: 81.9%; PPC: 82.3%; PPNC: 82.8%, **Table 4**). The persistence of these bands indicates that the β-1,4-glucosidic framework was retained as the principal structural feature after both the bleaching (7.5% NaOCl, 75 °C)

and the acid hydrolysis (64% H_2SO_4, 50 °C, 45 min) steps. This should be understood as evidence that the cellulose framework survived the treatments, and not as proof that no chain scission occurred, since FTIR band positions and relative intensities in this region are not sensitive to moderate reductions in degree of polymerization. Retention of the crystalline framework is nonetheless the property required for the production of cellulose nanocrystals, in which ordered domains must remain intact while amorphous regions are preferentially dissolved (Rezzouq et al., 2026; Tang et al., 2021).

Table 5. Crystallinity index (CI_FTIR) for pineapple peel materials.

Sample	Crystalline peak (cm^{-1})	Amorphous peak (cm^{-1})	CI_FTIR (mean ± SD)
PPP	1425	895	1.58 ± 0.04
PPC	1425	895	1.73 ± 0.03
PPNC	1425	895	1.91 ± 0.02

CI^{fjl} = Absorbance at 1425 cm^{-1} / Absorbance at 895 cm^{-1}. Values represent mean ± SD (n = 3 per sample). Higher CI indicates greater cellulose crystallinity.

Changes in hydrogen bonding and water content

The O-H stretching region (3600–3000 cm^{-1}) revealed a stepwise evolution across the three materials. The PPP spectrum exhibited a broad, low-transmittance peak at 3330 cm^{-1} (79.2%) characteristic of extensive hydrogen bonding in the amorphous cellulose matrix and associated non-cellulosic polymers. After alkaline and bleaching treatment, the PPC spectrum showed a narrower peak at 81.5% transmittance, indicating partial reduction in hydrogen bonding diversity due to the removal of hemicellulose and some lignin. The PPNC spectrum exhibited the sharpest peak at 83.1% transmittance as shown in **Table 4**. This was consistent with the selective removal of amorphous regions by acid hydrolysis. A complementary trend was observed at the O-H bending peak at 1630 cm^{-1} (PPP: 82.3%; PPC: 84.1%; PPNC: 86.0%, **Table 4**) which shows a progressive decrease in bound water across stages. This stepwise reduction in hydrogen bonding and bound water correlates with the physical properties data: moisture content declined from 8.83 ± 0.48% (PPP) to 5.08 ± 0.19% (PPC) and further to 3.75 ± 0.10% (PPNC) ($P < 0.001$, **Table 1**), and water absorption capacity decreased from 390 ± 1.41% to 171 ± 5.66% (PPC) and 201 ± 8.49% (PPNC) ($P < 0.001$, **Table 1**). The initial large drop from PPP to PPC in water absorption (56% reduction) reflects the removal of the highly hydrophilic hemicellulose and pectin fractions during alkaline treatment (Kamande et al., 2026; Li et al., 2021).

Changes in crystallinity

Crystallinity-related bands provided progressive evidence of structural ordering across the three samples (Gao et al., 2024). The CH_2 bending vibration at 1425 cm^{-1}, associated with cellulose crystallinity, changed stepwise from PPP (86.2%) to PPC (87.4%) to PPNC (88.9%) in transmittance terms (**Table 4** and **Fig. 3C**), while the β-glycosidic band at 895 cm^{-1}, associated with amorphous cellulose, changed from PPP (91.2%) to PPC (90.5%) to PPNC (89.1%). The resulting crystallinity index (CI_FTIR, **Equation 10**) increased from 1.58 ± 0.04 in PPP to 1.73 ± 0.03 in PPC and 1.91 ± 0.02 in PPNC (**Table 5**), indicating a greater proportion of ordered cellulose at each successive purification stage and consistent with selective removal of amorphous components. These values are of the same order as those reported by Abderrahim et al. (2015). Because the index is a ratio of two band absorbances rather than an absolute measurement, it should be interpreted as a relative indicator of structural order and not as a determination of absolute crystallinity, which would require X-ray diffraction (**Section 3.3**). The intermediate value obtained for PPC is consistent with its status as a cellulose-enriched material in which amorphous regions have been

partially disrupted but not yet selectively hydrolysed as in PPNC. The higher relative order of PPNC is the property that underpins its potential as a mechanical reinforcement in bio-based packaging films (Kaewprachu et al., 2026).

Correlation of FTIR results with other analytical findings

The FTIR results for all three samples correlate closely with the chemical composition data (Table 2) and the physical properties (**Table 1**). The stepwise reduction in the hemicellulose and lignin bands (**Table 4** and **Fig. 3A**) was matched by the progressive increase in cellulose content (PPP: 21.75%; PPC: 28.16%; PPNC: 32.22%) and the corresponding decrease in ash content (PPP: 5.90%; PPC: 4.11%; PPNC: 2.64%; **Table 2**). The FTIR difference spectrum (**Fig. 3B**) showed that the PPC–PPP deviations were intermediate between zero and the PPNC–PPP deviations, indicating that the purification stage is responsible for a meaningful but incomplete removal of non-cellulosic components. The O-H spectral changes (**Table 4**) aligned with the significant decrease in moisture content (PPP: 8.83%; PPC: 5.08%; PPNC: 3.75%; $P < 0.001$, **Table 1**) and in water absorption capacity (PPP: 390%; PPC: 201%; PPNC: 171%; $P < 0.001$, **Table 1**). The non-monotonic trend in water absorption, with the greatest reduction at PPC and a slight recovery in PPNC, is explained by the sulfate half-ester groups introduced during H_2SO_4 hydrolysis, which increase surface hydrophilicity despite the overall reduction in bound water (Imiete et al., 2023); this is corroborated by the relatively stable O-H region between PPC and PPNC in the difference spectrum (**Fig. 3B**). Taken together, these data indicate that the extraction protocol progressively transforms raw pineapple peel into a cellulose-enriched nanomaterial, with the purified intermediate (PPC) representing a distinguishable stage at which delignification and hemicellulose removal are already substantially advanced.

This study was limited by the unavailability of advanced characterization instruments, particularly Scanning Electron Microscopy (SEM) and X-ray Diffraction (XRD), during the experimental work. Consequently, the morphology, particle size distribution, and absolute crystallinity of the produced pineapple peel nanocellulose could not be comprehensively evaluated. FTIR spectroscopy was used as an alternative method to confirm structural changes and estimate relative crystallinity.

Conclusion

This study produced progressively purified cellulose-rich materials (PPP, PPC and PPNC) from the peel of Smooth Cayenne pineapple grown in Tanzania, using sequential chemical purification followed by sulfuric acid hydrolysis, and characterized the material at each of the three stages. Purification was evidenced by significant reductions in ash (5.90% to 2.64%), hemicellulose (16.66% to 12.08%) and lignin (11.69% to 6.06%), alongside an increase in cellulose content (21.75% to 32.22%) ($P < 0.01$). The stage-resolved design showed that hemicellulose removal was governed principally by the chemical purification step, whereas lignin removal proceeded significantly at both stages. The resulting PPNC combined a low moisture content (3.75%), a 48% lower water absorption capacity than the raw powder (201%) and a high water solubility index (90.75%), a combination that favors dispersion during solution casting while indicating that the moisture sensitivity of any resulting film requires experimental verification. These findings establish the peel of Tanzania-grown Smooth Cayenne pineapple as a viable, low-cost feedstock for nanocellulose production and provide the filler characterization on which the development of gellan gum-based biodegradable packaging films can proceed.

Acknowledgments

The research for this article was funded by FoodLAND project (Food and Local, Agricultural and Nutritional Diversity) which received support from the European Union's Horizon 2020 Research and Innovation program under grant agreement No. 862802.

Conflicts of interest

No potential conflict of interest was reported by the authors.

Disclaimer

Authors declare that NO generative AI technologies have been used during the writing or editing of this manuscript.

References

Abderrahim, B., Abderrahman, E., Mohamed, A., Fatima, T., Abdesselam, T., & Krim, O. (2015). Kinetic thermal degradation of cellulose, polybutylene succinate and a green composite: Comparative study. *World Journal of Environmental Engineering*, *3*(4), 95–110. https://doi.org/10.12691/wjee-3-4-1

Agarwal, J., Mohanty, S., & Nayak, S. K. (2020). Valorization of pineapple peel waste and sisal fiber: Study of cellulose nanocrystals on polypropylene nanocomposites. *Journal of Applied Polymer Science*, *137*(42), 49291. https://doi.org/10.1002/app.49291

Alves, A., Cisneros, E. F., Balmelli, G., Poltri, S. N. M., & Rodrigues, J. (2021). Assessment of eucalypts wood lignin content by analytical pyrolysis, comparison with Klason and total lignin contents. *Journal of Wood Chemistry and Technology*, *41*(6), 229–235. https://doi.org/10.1080/02773813.2021.1986071

AOAC. (2019). Official methods of analysis of AOAC International (21st ed.). *Maryland: AOAC International*.

Aththanayaka, S., Thiripuranathar, G., & Ekanayake, S. (2025). Sustainable approach for fabrication of pineapple agro-waste mediated cellulose nanocrystals embedded with Ag/Ag2O/ZnO nanocomposites for efficient removal of waterborne pathogens in wastewater. *International Journal of Biological Macromolecules*, *310*, 143272. https://doi.org/10.1016/j.ijbiomac.2025.143272

Barboza, L. G. A., Dick Vethaak, A., Lavorante, B. R. B. O., Lundebye, A. K., & Guilhermino, L. (2018). Marine microplastic debris: An emerging issue for food security, food safety and human health. *Marine Pollution Bulletin*, *133*, 336–348. https://doi.org/10.1016/j.marpolbul.2018.05.047

Barros, S. de S., Junior, W. A. G. P., Pereira, B., Mendoza, S. L. Y., Freitas, F. A. de, Saron, C., & Manzato, L. (2025). Extraction of cellulose nanofibrils and nanocrystals from a new cultivar of pineapple *(Ananas comosus* 'Vitória'*)* from the Amazon region. *Biofuels, Bioproducts and Biorefining*, *19 (6),* 1595-1610. https://doi.org/10.1002/bbb.2753.

Chong, W. T., Siow, L. F., Chan, E. S., Tey, B. T., & Lee, Y. Y. (2025). Enzymatic hydrolysis of palm cellulose to yield nanocrystals with potential roles in lipid and cholesterol digestion and absorption. *Cellulose,* 32(3), 1575-1595. https://doi.org/10.1007/s10570-025-06382-5

Dai, H., Ou, S., Huang, Y., & Huang, H. (2018). Utilization of pineapple peel for production of nanocellulose and film application. *Cellulose*, *25*(3), 1743–1756. https://doi.org/10.1007/s10570-018-1671-0.

Demircan, B., McClements, D. J., & Velioglu, Y. S. (2025). Next-generation edible packaging: development of water-soluble, oil-resistant, and antioxidant-loaded pouches for use in noodle sauces. *Foods*, *14*(6), 1061. https://doi.org/10.3390/foods14061061

Díaz-Montes, E. (2022). Polysaccharides: Sources, characteristics, properties, and their application in biodegradable films. *Polysaccharides*, *3*(3), 480–501. https://doi.org/10.3390/polysaccharides3030029.

Dutta, D., & Sit, N. (2024). A comprehensive review on types and properties of biopolymers as sustainable bio-based alternatives for packaging. *Food Biomacromolecules*, *1*(2), 58–87. https://doi.org/10.1002/fob2.12019.

Esquivel-Alfaro, M., Rojas-Carrillo, O., Sulbarán-Rangel, B., Rodríguez-Barquero, L., Palacios-Hinestroza, H., & Rojas, O. J. (2025). Pineapple-derived nanocellulose for nanocomposites: Extraction, processing, and properties. *Journal of Composites Science*, *9*(12), 652. https://doi.org/10.3390/jcs9120652

FAO. (2025). Crops and livestock products: Pineapple production quantity, United Republic of Tanzania, 2021 [Data set]. *Food and Agriculture Organization of the United Nations*. https://www.fao.org/faostat/en/#data/QCL

Fitriani, F., Aprilia, S., Arahman, N., Bilad, M. R., Amin, A., Huda, N., & Roslan, J. (2021). Isolation and characterization of nanocrystalline cellulose isolated from pineapple crown leaf fiber agricultural wastes using acid hydrolysis. *Polymers, 13*(23), 4188. https://doi.org/10.3390/polym13234188

Gao, D., Li, X., Li, F., Luo, R., Liao, H., & Man, J. (2024). Changes of crystalline structure and physicochemical properties of *Pueraria lobata* var. Thomsonii starch under water deficit. *Plos One*, *19*(7), e0304373. https://doi.org/10.1371/journal.pone.0304373

Henao Rodríguez, J. E., Escobar Rincón, D., Hincapié Rojas, D. F., Cely Orjuela, I. G., Socolovsky, L. M., Erazo Rondón, D. G., & Londoño Calderón, C. L. (2023). Effects of hydrolysis and bleaching conditions on the efficiency of cellulose microfibrils extraction from coffee parchment through a design of experiments. *Cellulose*, *30*(17), 10715–10731. https://doi.org/10.1007/s10570-023-05553-6

Hu, K., Hu, X., Zeng, L., Zhao, M., & Huang, H. (2010). Hydrogels prepared from pineapple peel cellulose using ionic liquid and their characterization and primary sodium salicylate release study. *Carbohydrate Polymers*, *82*(1), 62–68. https://doi.org/10.1016/j.carbpol.2010.04.023

Huang, Y.L., Chow, C.J., & Fang, Y.J. (2011). Preparation and physicochemical properties of fiber-rich fraction from pineapple peels as a potential ingredient. *Journal of Food and Drug Analysis*, *19*(3). https://doi.org/10.38212/2224-6614.2179

Imiete, I. E., Giannini, L., Tadiello, L., Orlandi, M., & Zoia, L. (2023). The effect of sulfate half-ester groups on the mechanical performance of cellulose nanocrystal-natural rubber composites. *Cellulose*, *30*(14), 8929–8940. https://doi.org/10.1007/s10570-023-05432-0

Jakrawatana, N., Ngammuangtueng, P., Vorayos, N., & Gheewala, S. H. (2023). Replacing single-use plastics with biomaterial packaging in Thailand and impacts on the water-energy-climate

Nexus. *Sustainable Production and Consumption*, *39*, 506–520. https://doi.org/10.1016/J.SPC.2023.05.036.

Kaewprachu, P., Klunklin, W., Jaisan, C., Rawdkuen, S., Sangsawad, P., Tongdeesoontorn, W., Kingwascharapong, P., & Kraithong, S. (2026). Comparative study of cellulose nanocrystals from young and mature coconut husks as reinforcement agents in sustainable gelatin-based films. *Polymers*, *18*(6), 708. https://doi.org/10.3390/polym18060708

Kamande, S. W., Kariuki, S. W., & Murithi, G. (2026). Impact of lignin on water absorption and thickness swelling of particleboard: A comprehensive review. *Advances in Materials Science and Engineering*, *2026*(1), 9065314. https://doi.org/10.1155/amse/9065314

Lee, D. S., & Robertson, G. L. (2021). Interactive influence of decision criteria, packaging film, storage temperature and humidity on shelf life of packaged dried vegetables. *Food Packaging and Shelf Life*, *28*, 100674. https://doi.org/https://doi.org/10.1016/j.fpsl.2021.100674

Li, M., He, B., Chen, Y., & Zhao, L. (2021). Physicochemical properties of nanocellulose isolated from cotton stalk waste. *ACS Omega*, *6*(39), 25162–25169. https://doi.org/10.1021/acsomega.1c02568

Li, X., Wan, C., Tao, T., Chai, H., Huang, Q., Chai, Y., & Wu, Y. (2023). An overview of the development status and applications of cellulose-based functional materials. *Cellulose*, *31*(1), 61–99. https://doi.org/10.1007/S10570-023-05616-8

Louis, A. C. F., Venkatachalam, S., & Gupta, S. (2022). Innovative strategy for rice straw valorization into nanocellulose and nanohemicellulose and its application. *Industrial Crops and Products*, *179*, 114695. https://doi.org/10.1016/j.indcrop.2022.114695

Madureira, A. R., Atatoprak, T., Cabuk, D., Sousa, F., Pullar, R. C., & Pintado, M. (2018). Extraction and characterisation of cellulose nanocrystals from pineapple peel. *International Journal of Food Studies*, *7*(1), 24–33. https://doi.org/10.7455/ijfs/7.1.2018.a3

Makaranga, A., Seth, M. S., Ndee, A., Mneney, E. E., Mbwambo, G., Lema, K., & Msogoya, T. J. (2018). Diversity and genetic identity of pineapple [*Ananas comosus* (L.) Merr.] in Tanzania based on microsatellite markers. *African Journal of Biotechnology*, 17(26), 811-817. https://doi.org/10.5897/ajb2018.16498

Mehraj, M., Das, S., Feroz, F., Waheed Wani, A., Dar, S. Q., Kumar, S., Wani, A. K., & Farid, A. (2024). Nutritional composition and therapeutic potential of pineapple peel – A comprehensive review. *Chemistry & Biodiversity*, *21*(5), e202400315. https://doi.org/10.1002/cbdv.202400315

Mohamed Al, H., ALSadi, H. L., & Hemalatha, K. (2025). Development and application of smart packaging solutions for extending the shelf life of fresh produce. In *SHS Web of Conferences* (Vol. 216, p. 01013). EDP Sciences. https://doi.org/10.1051/shsconf/202521601013

Nemeş, N. S., & Negrea, A. (2023). Infrared and visible spectroscopy: Fourier transform infrared spectroscopy and ultraviolet–visible spectroscopy. In Makarand M. Ghangrekar, Narcis M. Duteanu, Rao Y. Surampalli, Tian C. Zhang (Eds.), *Microbial Electrochemical Technologies: Fundamentals and Applications*, *1*, 163–200. https://doi.org/10.1002/9783527839001.ch6

Ngereza, A., Keutgen, A., & Pawelzik, E. (2007). Quality of mango, passion fruit and pineapple in Tanzania. *Utilisation of diversity in land use systems: Sustainable and organic approaches to meet human needs*. p. 165. Tropentag, Witzenhausen.

Pereira, P. H. F., Arantes, V., Pereira, B., Ornaghi Jr, H. L., De Oliveira, D. M., Santagneli, S. H., & Cioffi, M. O. H. (2022). Effect of the chemical treatment sequence on pineapple peel fiber: Chemical composition and thermal degradation behavior. *Cellulose*, *29*(16), 8587–8598. https://doi.org/10.1007/s10570-022-04806-0

Prado, K. S., & Spinacé, M. A. S. (2019). Isolation and characterization of cellulose nanocrystals from pineapple crown waste and their potential uses. *International Journal of Biological Macromolecules*, *122*, 410–416. https://doi.org/10.1016/j.ijbiomac.2018.10.187

Qureshi, S. S., Nizamuddin, S., Xu, J., Vancov, T., & Chen, C. (2024). Cellulose nanocrystals from agriculture and forestry biomass: synthesis methods, characterization and industrial applications. *Environmental Science and Pollution Research,* 31(49), 58745-58778. https://doi.org/10.1007/s11356-024-35127-3

Rahayu, A., Hanum, F. F., Amrillah, N. A. Z., Lim, L. W., & Salamah, S. (2022). Cellulose extraction from coconut coir with alkaline delignification process. *Journal of Fibers and Polymer Composites*, *1*(2), 106–116. https://doi.org/10.55043/jfpc.v1i2.51

Rezzouq, A., Belfadil, D., Bouftou, A., Fettah, I., Bouchti, M. E., Cherkaoui, O., Zyade, S., & Majid, S. (2026). Extraction and characterization of cellulose nanocrystals from post-harvest of melon plant residues: A new sustainable source of cellulose. *Scientific African*, *31*, e03242. https://doi.org/10.1016/j.sciaf.2026.e03242

Romruen, O., Kaewprachu, P., Karbowiak, T., & Rawdkuen, S. (2022). Isolation and characterization cellulose nanosphere from different agricultural by-products. *Polymers*, *14*(13), 2534. https://doi.org/10.3390/polym14132534

Santos, R. M. dos, Neto, W. P. F., Silvério, H. A., Martins, D. F., Dantas, N. O., & Pasquini, D. (2013). Cellulose nanocrystals from pineapple leaf, a new approach for the reuse of this agro-waste. *Industrial Crops and Products*, *50*, 707–714. https://doi.org/10.1016/j.indcrop.2013.08.049

Sengar, A. S., Sunil, C. K., Rawson, A., & Venkatachalapathy, N. (2022). Identification of volatile compounds, physicochemical and techno-functional properties of pineapple processing waste (PPW). *Journal of Food Measurement and Characterization*, *16*(2), 1146–1158. https://doi.org/10.1007/s11694-021-01243-8

Tang, L., Liao, J., Dai, H., Liu, Y., & Huang, H. (2021). Comparison of cellulose nanocrystals from pineapple residues and its preliminary application for Pickering emulsions. *Nanotechnology*, *32*(49), 495708. https://doi.org/10.1088/1361-6528/ac21f1

Teklemedhin, T. B., Ahmad, R., Li, M., Zhang, B., Guo, Y., Niu, M., & Li, H. (2026). Cellulose nanocrystal/chitosan hybrid bio-composite films for food packaging application: A review on synthesis, mechanisms and functional properties. *Food Reviews International*. *42*(6), 4481-4509. https://doi.org/10.1080/87559129.2026.2631780

Wahyudi, M. S., Holilah, Bahruji, H., Prasetyoko, D., Asranudin, Pratama, A. W., Indriani, D. W., Suryanegara, L., Faradilla, R. F., Mahardika, M., Wardani, R. K., Piluharto, B., Knight, V. F., & Norrrahim, M. N. F. (2025). The effect of organic acid hydrolysis on the properties of nanocellulose from edamame husk (*Glycine max* (L.) merill). *Case Studies in Chemical and Environmental Engineering*, *11*, 101179. https://doi.org/10.1016/j.cscee.2025.101179

Zhao, X., Cornish, K., & Vodovotz, Y. (2020). Narrowing the Gap for Bioplastic Use in Food Packaging: An Update. *Environmental Science & Technology*, *54*(8), 4712–4732. https://doi.org/10.1021/acs.est.9b03755